DOI: https://doi.org/10.24425/amm.2026.1973

MACIEJ MOTYKA[1,2*], ANNA BARAN-SADLEJA[2,3], WITOLD CHROMIŃSKI[4], TOMASZ TOKARSKI[5]

MICROSTRUCTURAL CHARACTERIZATION OF THE EFFECT OF MINOR AND SEVERE PLASTIC DEFORMATION ON MARTENSITE DECOMPOSITION IN Ti-6Al-4V ALLOY

Martensite decomposition in titanium alloys is the phase transformation most commonly associated with their standard heat treatment – hardening and tempering. However, it also occurs during other manufacturing processes, such as thermomechanical processing and additive manufacturing. Understanding the nature of the martensite decomposition process enhances the ability to control it. Unlike previous studies in this field, which were based on light microscopy (LM) and scanning electron microscopy (SEM) analysis, this study examined the effect of plastic deformation of martensite on its decomposition using transmission electron microscopy (TEM) and EBSD/TKD methods. In addition, a variant of hydrostatic extrusion of the quenched Ti-6Al-4V alloy was also considered.

Keywords: Titanium alloys; Martensite decomposition; Plastic deformation; Transmission electron microscopy (TEM); Electron Backscattered Diffraction (EBSD); Transmission Kikuchi Diffraction (TKD)

1. Introduction

Titanium alloys are characterized primarily by high specific strength and corrosion resistance, which makes them suitable for use in many sectors of the economy, including strategic sectors such as the aerospace and defense industries. One of the most commonly used is Ti-6Al-4V, which belongs to the group of martensitic alloys. Its mechanical properties, which determine its applications, are achieved through hot working and heat treatment processes, including hardening and tempering operations.

Martensitic transformation in titanium alloys occurs during quenching from the temperature range of stable β phase at the high cooling rate or plastic deformation. It results from allotropic transformation Tiα ↔ Tiβ, which is considered as a primary phase transformation in titanium. During the cooling from the temperature above 882.5°C, Tiβ form (bcc) transforms into Tiα form (hcp). At the low cooling rates, allotropic transformation Tiβ → Tiα proceeds by nucleation and growth of new phase crystals, whereas at the high cooling rate, the allotropic transformation has features of martensitic transformation. Increase in alloying elements (e.g. Cr, Mo, V, Nb, Sn and Zr) in two-phase α + β titanium alloys, reduces significantly the martensite start temperature (T_{MS}) and fully martensitic microstructure in these alloys can be developed. In titanium alloys containing Mo, Mn, Nb and V, martensitic transformation can be induced by plastic deformation caused by external load. Main martensitic phases – α' and α'' – are the supersaturated solid solutions of the alloying elements in Tiα. Martensitic α' phase crystallizes in the hexagonal structure while α'' phase in the orthorhombic one. The α'' phase is formed in titanium alloys containing transition elements. Both of them have a similar morphology – α'' phase laths are smaller in size compared to the laths of α' phase. Their distinction quite often is difficult (the transition from one phase to another with the change of concentration of the elements in solid solution) therefore they are usually considered as a single martensitic phase – α'(α'') [1-3].

Usually, the content of martensitic phases in the microstructure of structural alloys are not advisable. Their final mechanical properties are achieved after tempering, leading to martensite decomposition. Based on literature data [4-7], the martensitic crystals of metastable α' and α'' phases decompose into a mix-

1 RZESZÓW UNIVERSITY OF TECHNOLOGY, DEPARTMENT OF MATERIALS FORMING AND PROCESSING, 8 POWSTANCOW WARSZAWY AV., 35-029 RZESZOW, POLAND
2 RZESZÓW UNIVERSITY OF TECHNOLOGY, DEPARTMENT OF MATERIALS SCIENCE, 4 ZWIRKI I WIGURY STR., 35-036 RZESZOW, POLAND
3 MTU AERO ENGINES POLSKA, TAJECINA 108, 36-002 JASIONKA, POLAND
4 WARSAW UNIVERSITY OF TECHNOLOGY, FACULTY OF MATERIALS SCIENCE AND ENGINEERING, 141 WOLOSKA STR., 02-507 WARSZAWA, POLAND
5 AGH UNIVERSITY OF KRAKOW, ACADEMIC CENTRE FOR MATERIALS AND NANOTECHNOLOGY, 30 KAWIORY STR., 30-055 KRAKOW, POLAND

* Corresponding author: motyka@prz.edu.pl

ture of α and β phases (α+β), according to the following general formula (1):

$$\alpha' \rightarrow \alpha'_{depl} + \beta \rightarrow \alpha + \beta \text{ and } \alpha'' \rightarrow \alpha''_{enr} + \\ + \alpha_M \rightarrow \alpha + \beta_M \rightarrow \alpha + \beta \quad (1)$$

where: α'_{depl} – α' phase depleted of alloying elements stabilizing β phase, α''_{enr} – α'' phase enriched of the alloying elements stabilizing β phase, α_M and β_M – metastable phases.

The efficiency of martensite decomposition in titanium alloys depends on the process temperature and time. Referring to the above equation (1), the expected high strength after tempering results from the formation of metastable phases, their decomposition and precipitation of highly dispersed phases. It should be noted that the martensitic phases (α', α'') decomposition can be assisted by creation of metastable phases (e.g. Ti_3Al) as well [8,9].

The heat treatment by hardening and tempering has long been used for structural titanium alloy. Therefore the martensite decomposition seems not to be an important phenomena, worth to be extensively investigated nowadays. However, it turns out that the new technologies introduced – e.g. 3D printing – have restored the need of further research in this area. The martensite decomposition has become again up-to-date because of additive methods development – produced parts made of titanium alloys (e.g. Ti-6Al-4V) are characterized by reduced ductility caused by the content of martensitic phases in their microstructure [10-12].

Moreover, decomposition process cannot be joined with tempering operation only. Exemplary, the martensite decomposition in Ti-6Al-4V alloy plays crucial role in the first stage of its superplastic deformation [13,14]. Additional research on this alloy [4] revealed differences between martensite decomposition process in static and dynamic (during deformation at 900°C).

Limited number of publications refer to the possibility of plastic deformation of titanium alloys in hardened state [15]. Illarionov et al. [16] provided some information about decomposition of cold deformed martensite in Ti–3Al–4.5V–5Mo (VT16) alloy. They reported that α'' phase, formed during quenching, can transform to α' phase during the tempering and indicated some differences in kinetics of decomposition process of undeformed and deform martensite phases.

In previous investigation [17] water quenched, and subsequently cold deformed Ti-6Al-4V alloy was tempered at the temperature range of 600-900°C for 1 and 2 h. It was revealed by light and scanning electron microscopy observations that the plastic deformation on tempered martensite laths influenced their morphology – particularly at the temperature of 900°C wherein fragmentation and spheroidization processes were identified. Based on hardness results, it was found that martensite α'(α'') underwent hardening – hardness and proof stress of quenched and cold deformed Ti-6Al-4V alloy was higher about 10% and 30% comparing with undeformed one, respectively. Obtained results of preliminary investigations indicated the necessity of using additional advanced research methods – including transmission electron microscopy (TEM).

Recent paper on research involving TEM examination (supported by synchrotron radiation facilities) refers to the decomposition kinetics of α'' martensite in Ti-6Al-6V-2Sn alloy during continuous heating [18]. Its authors revealed that decomposition of supersaturated α'' phase at the temperature range of 400-600°C is a diffusion-driven process. Experimental methods used in research enabled to found that decomposition of α'' martensite is preceded by nano-twinning of α'' laths – caused most likely by stress concentrations associated with structural heterogeneities. The paper provides also some details on microstructural mechanism of martensite decomposition. It was stated that β phase can be formed through two ways:

- precipitations of fine β particles (with diameter of ~5 nm) were formed mainly along the boundaries of α'' (during the first stage of α'' phase decomposition);
- β phase was also identified in the interior of highly twinned α'' by segregation of β stabilizing elements in these regions.

Martensite decomposition was also investigated in electron beam melt Ti-6Al-4V alloy [19]. The α' was the only martensite phase in the alloy microstructure which decomposed into α + β microstructure. Using atom probe tomography technique, the interphase boundaries α/β were studied. It was also found that the martensite decomposition is a diffusion-driven process leading to the transformation α' laths into α laths and β phase formation on their boundaries. Authors, based on TEM results, indicates twins and stacking faults in α' laths but they did not considered their role in martensite decomposition process.

The current research, resulting from previous investigation on the effects of plastic deformation on martensite decomposition in Ti-6Al-4V alloy, refers to TEM and SEM observations revealing details of martensite microstructure. It was intended to describe the influence of substructure components of martensite phase on its decomposition at the temperature range of 600-900°C. Additionally, an innovative approach is the evaluation of deformation method effect on decomposition process – therefore besides cold compressed samples the hydrostatically extruded water quenched Ti-6Al-4V alloy was analysed too.

2. Material and methods

Two-phase α + β Ti-6Al-4V titanium alloy (Al – 6.78, V – 4.38 Fe – 0.18, Si – 0.33 wt. % – Ti – balance) in the form of bars with 8 mm diameter. Cylindrical samples (ϕ = 8 mm, h = 10 mm) cut by EDM method were water quenched (WQ) from the temperature of 1050°C (stable β phase range) after 20 min annealing and tempered (T) at the temperature of 600, 750 and 900°C for 1 and 2 h. Some WQ samples were cold compressed (CC) before tempering, using Instron 5982 testing machine at the cross-head velocity of 1 mm/min up to rupture (strain about 10% – [17]). The present study includes another method of plastic deformation – hydrostatic extrusion (HE). WQ sample was severely plastically deformed in a single-pass HE process at the temperature of 600°C (in the Institute of High Pressure Physics UNIPRESS of Polish Academy of Science – [20]). Due to relative high deformation temperature and the lack significant microstructural changes at the tempering temperature of 600 and 750°C for examined material [17], hydrostatically extruded alloy was tempered at 900°C for 1 and 2 h.

Microscopic observations of the longitudinal surface of cylindrical samples were conducted using:

– light microscope (LM) Nikon Epihot 300 – in brightfield mode and using Nomarski contrasts (DIC),
– scanning electron microscope (SEM) Hitachi S-3400N equipped with energy dispersive spectrometer (EDS),
– scanning transmission electron microscope (SEM/STEM) Hitachi S-5500 equipped with EDS detector,
– transmission electron microscope (TEM) JEOL JEM 1200EX II operated at 120kV.

Discs 0.2 mm thick were cut using the electric discharge machining method and then polished using a Gatan Dimple Grinder. Thin films were prepared by electrolytic thinning (35 V) in a solution of perchloric acid in methanol (with a dilution ratio of 1:9).

For transmission Kikuchi diffraction (TKD) analysis (also called transmission electron backscatter difraction – tEBSD)), an FEI Versa 3D microscope (accelerating voltage 30 kV) equipped with an Oxford Symmetry S2 detector was used, with a sample tilt of –20° and a resolution of 200 nm.

Vickers hardness was measured using Innovatest Nexus 4303 tester with test force of 2.942N.

3. Results and discussion

3.1. Water quenching and plastic deformation

The microstructure of examined Ti-6Al-4V titanium alloy in its as-delivered condition – i.e., after hot rolling – is two-phase, consisting of primary α phase grains – elongated in the longitudinal direction of the bar – embedded in a matrix of the transformed β phase (a mixture of the β phase and fine precipitates of the secondary α phase) (Fig. 1a). As a result of water quenching within the temperature range of the stable β phase, a martensitic microstructure was obtained (Fig. 1b,c) – needle-like laths of the α’(α”) phase within the grains of the primary β phase (Fig. 1b). After cold compression test of WQ Ti-6Al-4V alloy, no change in the shape of the primary β beta phase grains was observed (Fig. 2a). However, the curvilinear shape of the needle-like martensite laths could suggest their deformation (Fig. 2b). The microstructure of the Ti-6Al-4V alloy, hydrostatically extruded at 600°C, retained its martensitic character (Fig. 3b).

TEM microscopic examinations of the Ti-6Al-4V alloy in the quenched state revealed dislocation substructures of varying densities (Fig. 3a), formed during cooling as a result of high thermal stresses. The tendency of martensite laths to twinning was also demonstrated (Fig. 3b).

No effect of plastic deformation on the dislocation density in martensite laths (Fig. 4) was observed compared to undeformed martensite (Fig. 3). Twin boundaries (Fig. 4a) with a morphology similar to that in undeformed martensite (Fig. 3b) were identified in the martensite laths, as well as those that were more densely distributed and significantly smaller in size, which

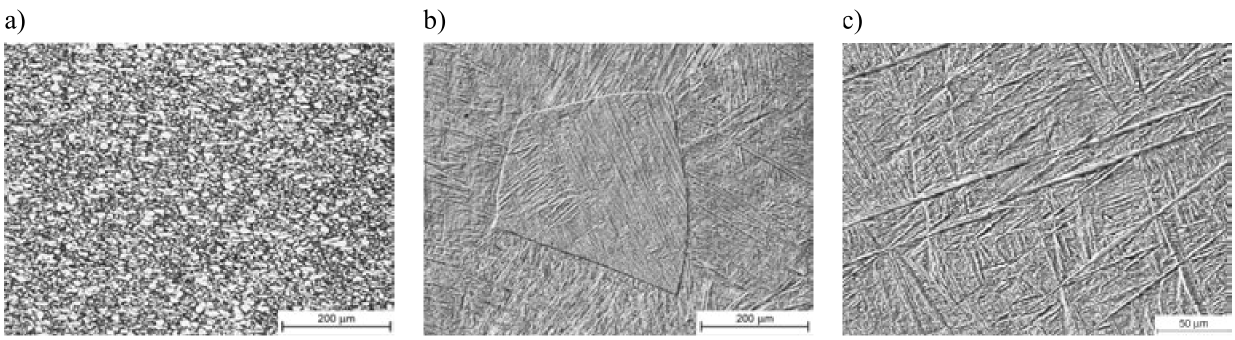

Fig. 1. Microstructure (LM) of Ti-6Al-4V alloy: as-received (a) and WQ (b,c – DIC)

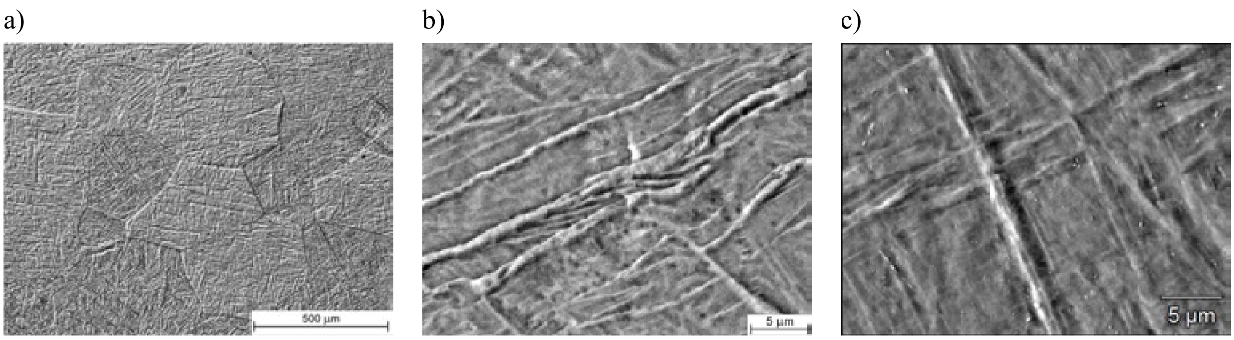

Fig. 2. Microstructure of Ti-6Al-4V alloy: WQ + CC (a,b) and WQ + HE (c) – a) LM/DIC, b,c) SEM

a) b)

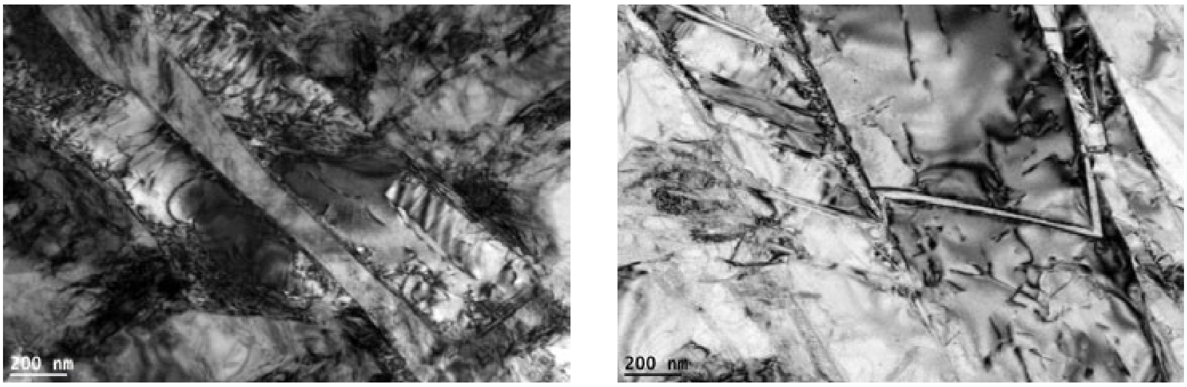

Fig. 3. Microstructure (TEM) of WQ Ti-6Al-4V alloy – dislocation substructure (a) and twins (b) in martensite laths

a) b)

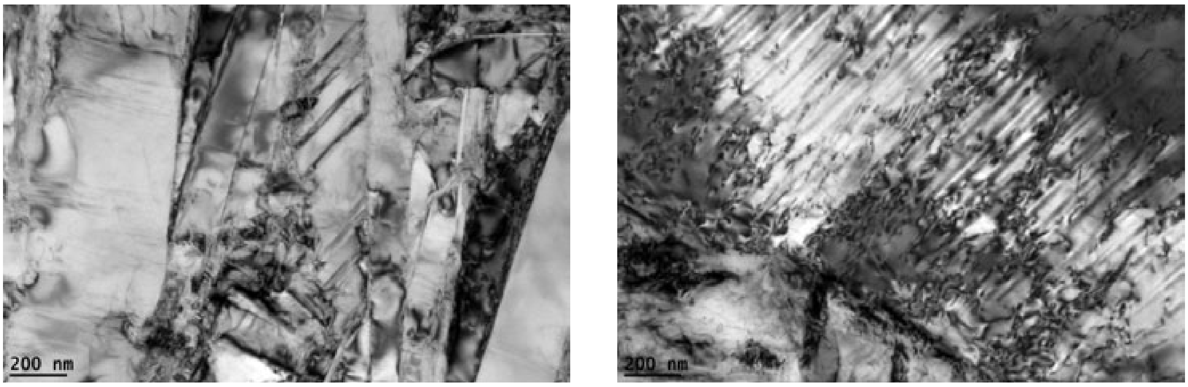

Fig. 4. Microstructure (TEM) of WQ + CC Ti-6Al-4V alloy – twins in fine (a) and coarse (b) cold deformed martensite laths

appears to be a characteristic feature of cold deformed martensite (Fig. 4b). E. Farbi et al. [21] refer to such defects in the quenched Ti-6Al-4V alloy as transformation twins.

Studies of water quenched and hydrostatically extruded Ti-6Al-4V titanium alloy have made it possible to expand the analysis of the effect of deformation at elevated temperatures on martensite decomposition to include the mode of deformation. Hydrostatic extrusion, apart from a significantly higher degree of plastic deformation – the actual strain in a single extrusion pass at 600°C is 1.4 – s characterized by a different, more complex state of deformation compared to a compression test. The HE process is also carried out at a significantly higher strain rate (approx. 10 s^{-1} – for a pressing speed of 40 mm/s). Such a short deformation time, despite the elevated temperature (possibly higher than the nominal temperature due to the thermal effect of deformation), does not cause a change in the morphology of the microstructural components typical of the quenched state (Fig. 5a), although areas with a completely different morphology have been identified (Fig. 5b). The difference in the degree of defect formation in the crystalline structure of the martensite

a) b)

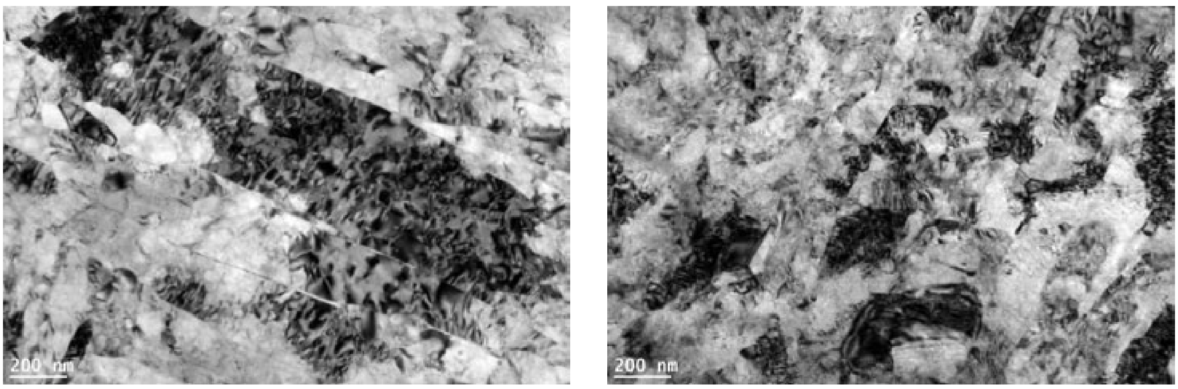

Fig. 5. Microstructure (TEM) of WQ + HE Ti-6Al-4V alloy – dislocation substructure in lath-like (a) and non-lath-like hydrostatically extruded martensite

laths in all these cases is difficult to determine, however, no twins were identified after the HE process.

STEM/EDS analysis revealed the chemical homogeneity of martensite, both in the undeformed state (Fig. 6a) and after cold deformation (Fig. 6b) and hydrostatic extrusion (Fig. 6c).

3.2. Tempering of undeformed and deformed martensite

Previously published SEM analysis results [17] showed that tempering the Ti-6Al-4V alloy at 600°C for 1 and 2 hours leads to the thickening of α-phase laths formed from both undeformed and deformed martensite. The use of transmission electron microscopy confirmed the preservation of the lath-like morphology of α-phase (Fig. 7a, c, d). In the laths formed from undeformed martensite, very fine precipitates (several nanometers in size) were observed (Fig. 7b), with a characteristic triangular morphology. The formation of nanometer-sized Ti_3Al phase precipitates under these conditions cannot be ruled out [22-24]. It was found that the α-phase laths, particularly in the WQ + CC alloy, are separated by a nanometer-sized (<100 nm) layer of the β-phase (Fig. 7c,d). Characteristic of the laths formed from deformed martensite are lattice defects – especially for very thin (<300 nm) ones (Fig. 7c,d).

Tempering at 750°C for 1 and 2 hours leads to further thickening of the α-phase laths and the formation of a β-phase between them (Fig. 8). The lath-like nature of the alloy's microstructure is preserved, both in the case of tempering after WQ and in the case of WQ+CC.

During tempering at 900°C, the thickness of the α-phase laths increases to ≥1 μm (Fig. 9a). Dislocations appear to play an important role in shaping the microstructure at this temperature, forming characteristic substructures – transforming into small-angle grain boundaries (SAGB's) in the laths formed as a result of the decomposition of deformed martensite (Fig. 9b). The tendency toward fragmentation and spheroidization of α-phase laths was previously demonstrated using LM and SEM methods in [17].

In the HE Ti-6Al-4V alloy, tempering at 900°C (for both 1 and 2 hours) leads to more intense spheroidization of the α phase (Fig. 10a) – elongated α phase grains were practically not observed. The matrix of these grains is a transformed β phase with a lamellar morphology, and twins form in the lamellae of the secondary α phase (Fig. 10b). The significant volume fraction of the transformed β phase is a characteristic feature of the hydrostatically extruded alloy tempered at 900°C, which was not observed after tempering of the quenched or quenched and plastically deformed material in a compression test at room temperature (Fig. 9). The applied temperature of 900°C is already within the α + β → β phase transformation temperature range. Therefore, it can be assumed that the greater degree of deformation in the HE process promotes the formation of the β phase at the tempering temperature of 900°C, which transforms into a mixture of α and β lamellae – i.e., the transformed β phase – during cooling.

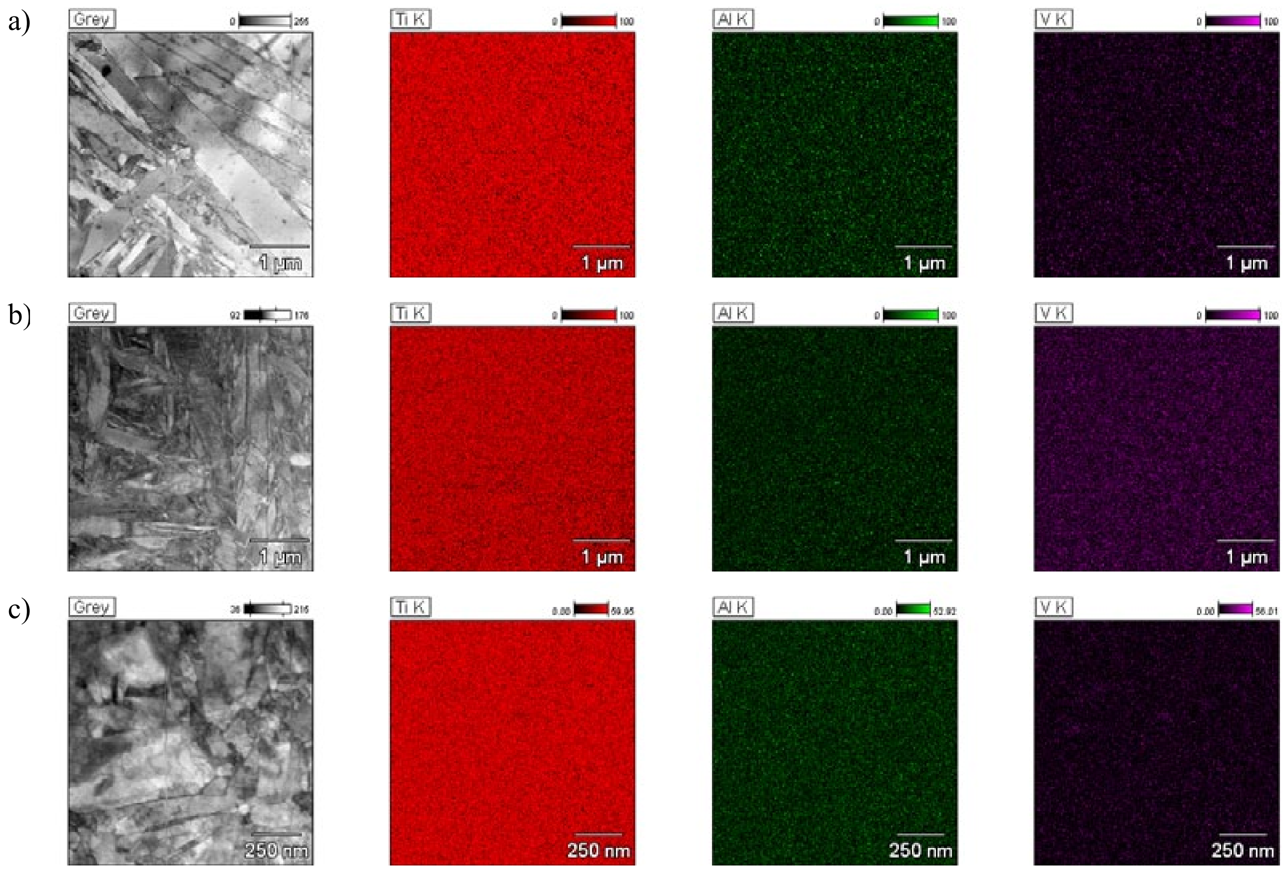

Fig. 6. Microstructure (STEM) of Ti-6Al-4V alloy: a) WQ, b)WQ + CC, c) WQ + HE – Ti, Al and V distribution maps (EDS)

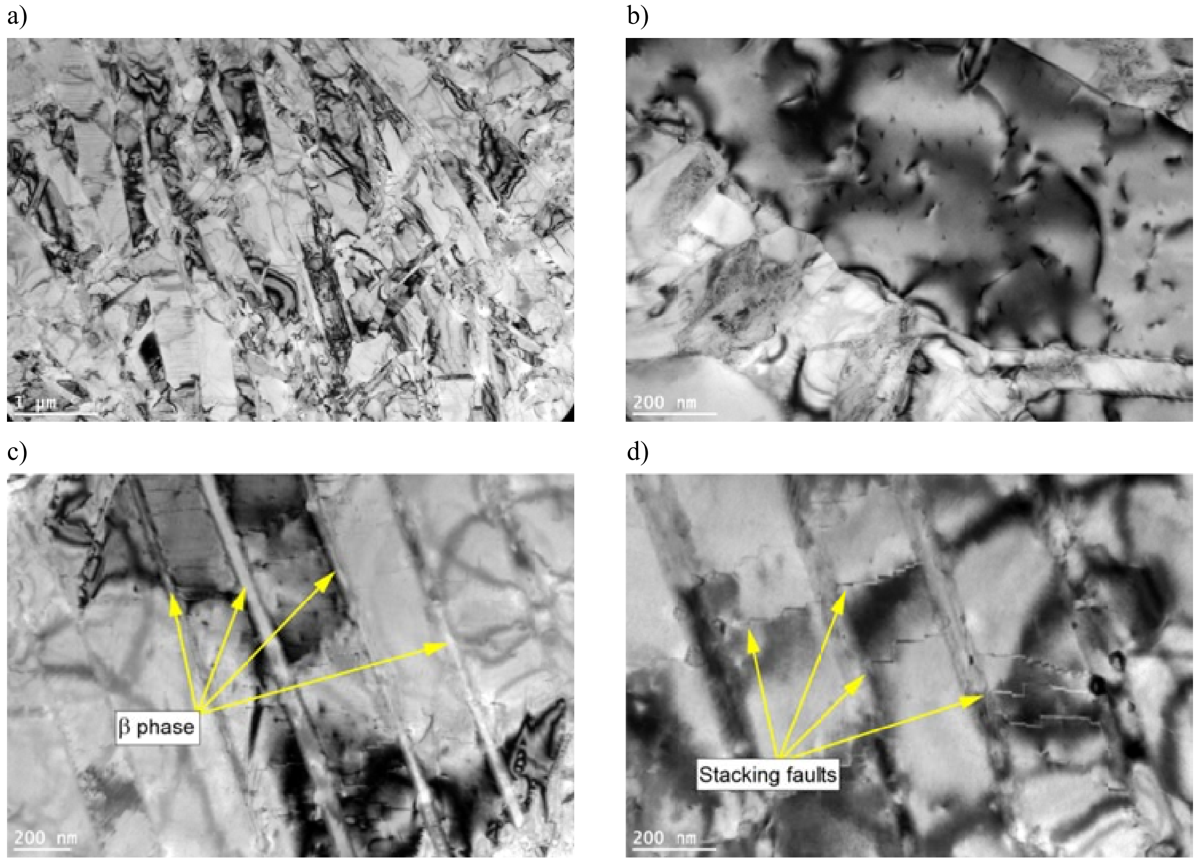

Fig. 7. Microstructure (TEM) of WQ (a,b) and WQ + CC (c,d) Ti-6Al-4V alloy after tempering at 600°C for 2 hours – a) morphology of tempered martensite laths, b) precipitates in tempered martensite lath, c) β-phase in the form of layers between tempered cold deformed martensite laths, d) stacking faults in tempered cold deformed martensite laths

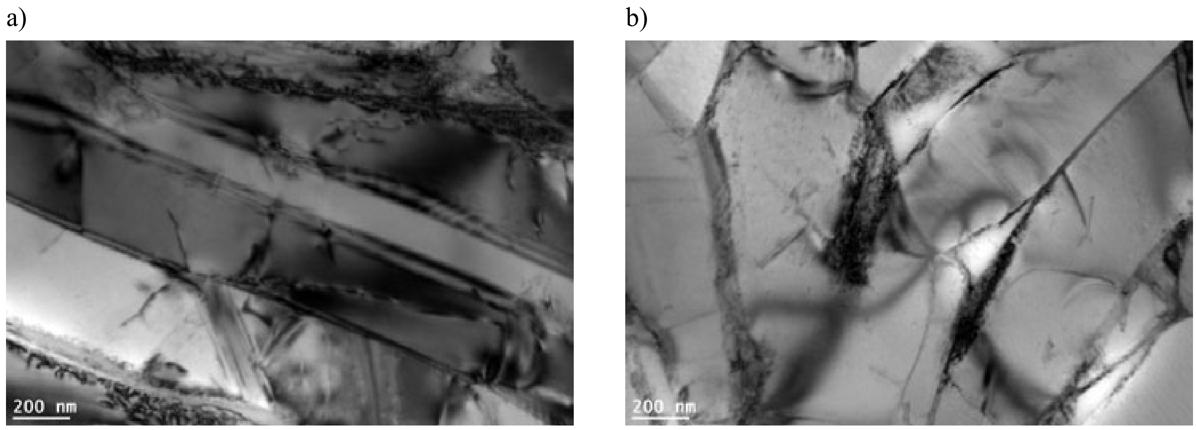

Fig. 8. Microstructure (TEM) of WQ (a) and WQ + CC (b) Ti-6Al-4V alloy after tempering at 750°C for 2 hours – morphology of β-phase between α-phase laths formed from undeformed (a) and cold deformed (b) martensite

The results of the STEM/EDS analysis indicate that the diffusion of alloying elements plays a significant role in the microstructure formation of the tempered Ti-6Al-4V alloy. Tempering is associated with a reduction in the degree of martensite supersaturation, particularly with respect to the element stabilizing the β phase – i.e., V. Vanadium, diffusing outward from the α'(α") phase laths, contributes to the formation of the β phase between them (Fig. 11). The concentration of Al, as an α-phase stabilizer in titanium alloys, is higher in the α laths.

3.3. TKD analysis

Titanium alloys, despite the difficulty of sample preparation, are studied using EBSD methods, but more often in terms of the difference in grain orientation between the α and β phases [25], phase identification in a lamellar microstructure [26], or grain size determination – particularly in the case of a UFG microstructure [27]. Martensitic microstructure is less frequently analyzed by the EBSD method – using significantly

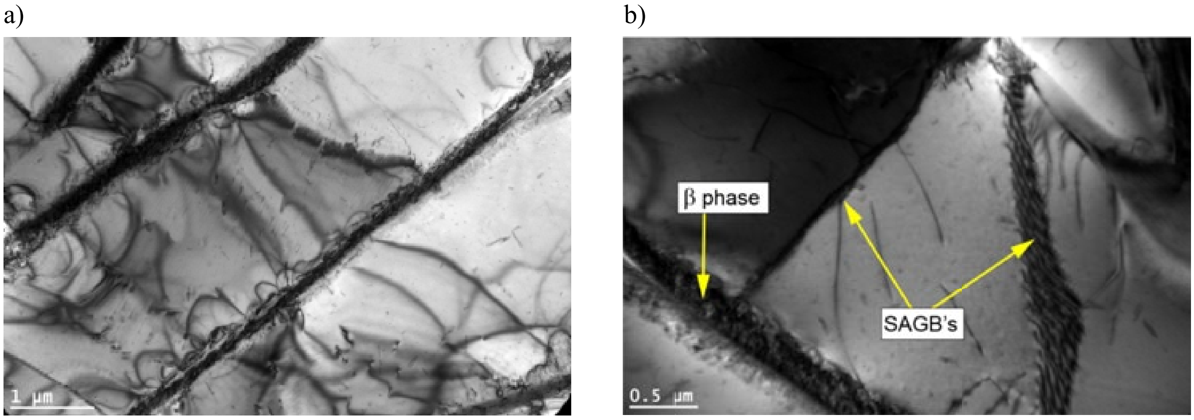

Fig. 9. Microstructure (TEM) of WQ (a) and WQ + CC (b) Ti-6Al-4V alloy after tempering at 900°C for 2 hours – dislocation substructure and SAGB's in α-phase laths formed from undeformed (a) and cold deformed (b) martensite

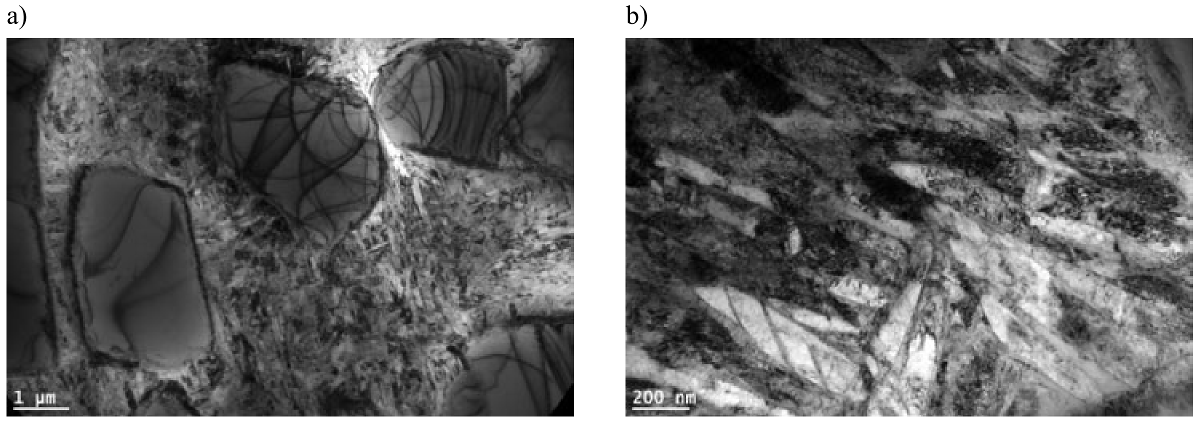

Fig. 10. Microstructure (TEM) of WQ + HE Ti-6Al-4V alloy after tempering at 900°C for 2 hours – a) globular α phase in the matrix of transformed β-phase, b) lamellar morphology of transformed β-phase

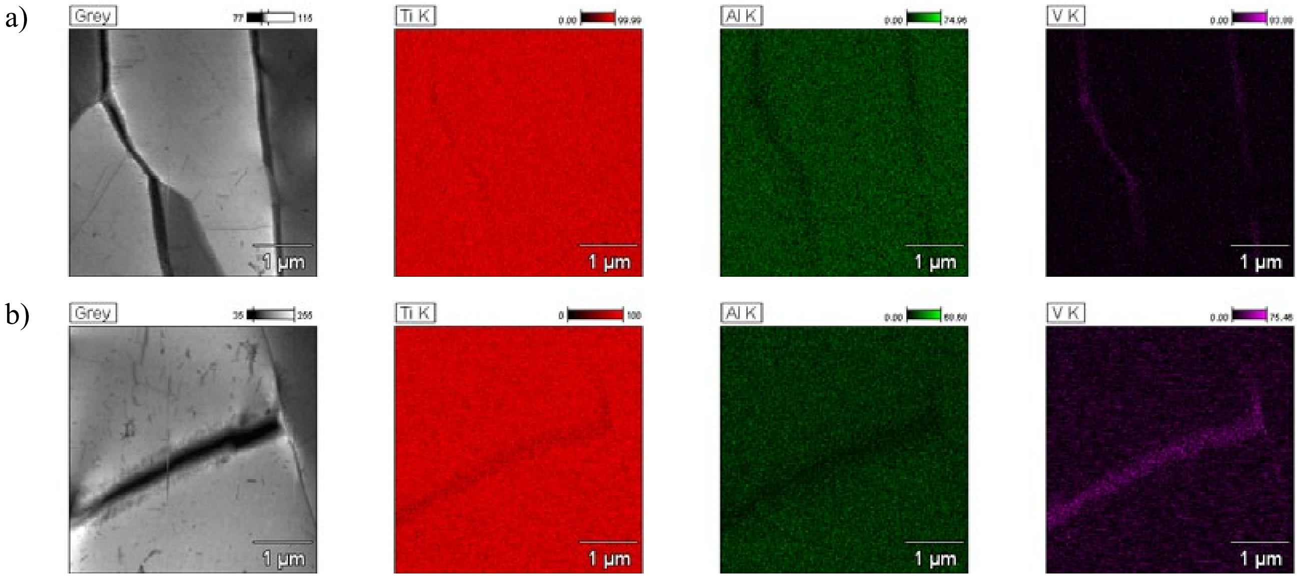

Fig. 11. Microstructure (STEM) of Ti-6Al-4V alloy tempered at 900°C for 2 hours after: a) WQ, b)WQ + CC – Ti, Al and V distribution maps (EDS) confirming the presence of the b β phase at the grain boundaries of the α phase

lower magnification to evaluate the grains of the primary β phase [28]. In the presented studies of the Ti-6Al-4V alloy, the classical EBSD method was used. Due to the poor quality of the IPF maps obtained by the classical EBSD method, their use was discontinued, and further analysis was performed using the EBSD/TKD method.

The IPF maps obtained using the TKD method showed that the parallel martensite laths have a similar crystallographic orientation, both in the (Fig. 12a) and in the quenched and then plastically deformed state (Fig. 12c). Analysis of the detector data indicates a significant increase in the proportion of SAGB's (2-10°) – from 4.35% for the quenched state (Fig. 12b) to 31.7% after deformation (Fig. 12d). It can be assumed that the essence of the effect of plastic deformation at room temperature on martensite laths in the Ti-6Al-4V alloy is the reorganization of crystal defects into SAGB's. However, this effect may be local in nature – results obtained at higher magnification for the alloy tempered at 600°C do not confirm this assumption (Fig. 13).

Tempering at 750°C leads to a change in the morphology of the α-phase laths – their thickness increases, while the degree of elongation and the straightness of the boundaries decrease, regardless of the plastic deformation of the martensite (Fig. 14).

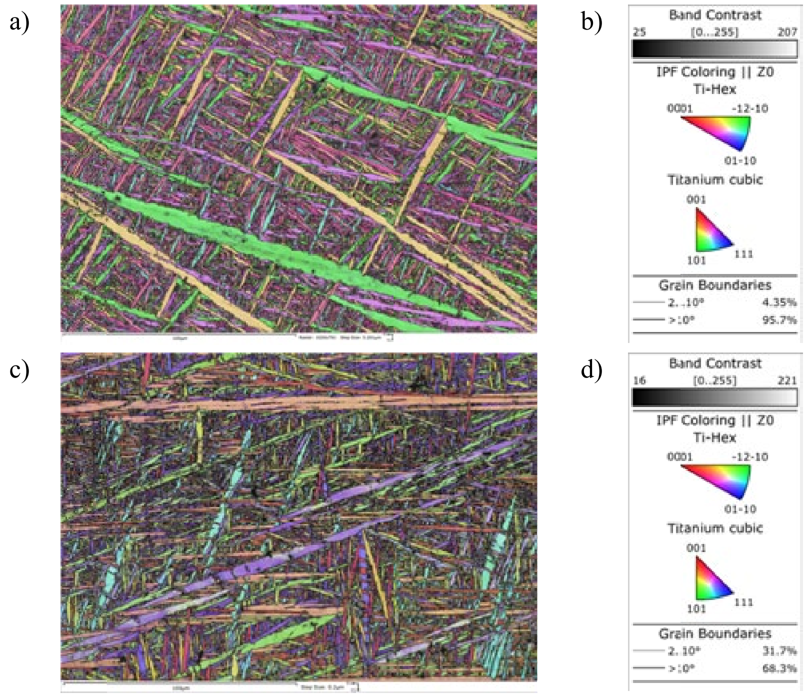

Fig. 12. EBSD/TKD-IPF orientation maps for α laths in Ti-6Al-4V alloy tempered at 750°C for 2 hours, following after WQ (a) and WQ + CC (c) – b,d) IPF color schemes for α'(α") and β phases

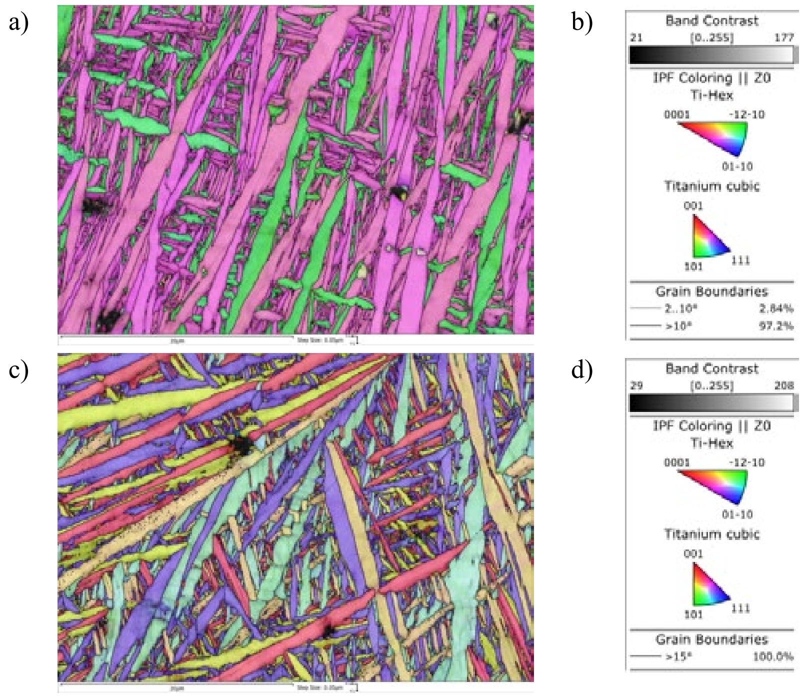

Fig. 13. EBSD/TKD-IPF orientation maps for α phase laths in Ti-6Al-4V alloy tempered at 600°C for 2 hours after WQ (a) and WQ + CC (c) – b,d) IPF color schemes for α and β phases

a) b)

c) d)

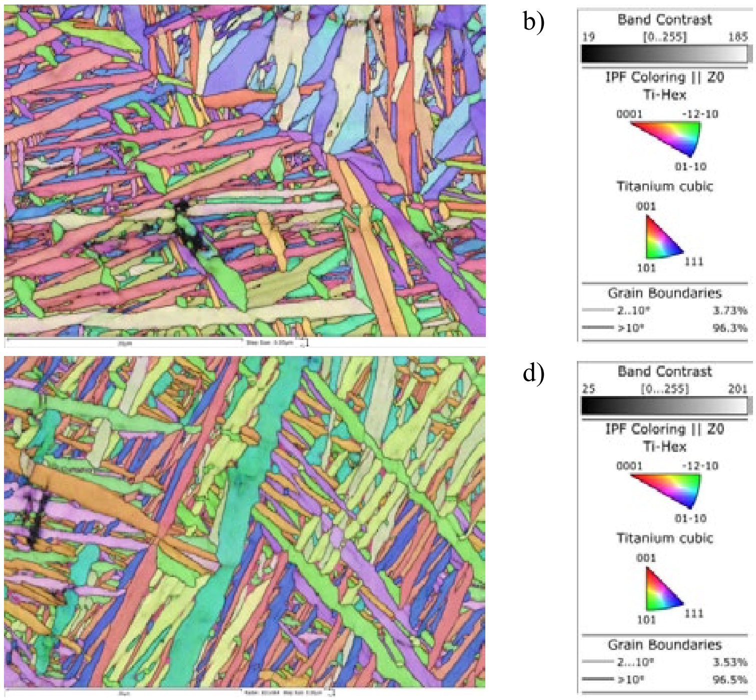

Fig. 14. EBSD/TKD-IPF orientation maps for α phase laths in Ti-6Al-4V alloy tempered at 750°C for 2 hours after WQ (a) and WQ + CC (c) – b,d) IPF color schemes for α and β phases

The effect of deformation became apparent after tempering at 900°C. In the undeformed and tempered states, the laths appear to retain the crystallographic orientation of martensite (Fig. 15a). After WQ + CC, the laths undergo fragmentation and spheroidization (Fig. 15c). Phase composition maps (Fig. 16) confirmed that after tempering at 750 and 900°C, a β phase forms between the α phase crystallites.

3.4. Hardness

The Ti-6Al-4V titanium alloy used in the study, in its as-delivered condition, exhibits a hardness of 342 HV. Hardness measurement results (Fig. 17) also indicate that water quenching from a temperature within the stable β phase range (1050°C) causes an increase in its hardness to 373 HV. After a compression test at

a) b)

c) d)

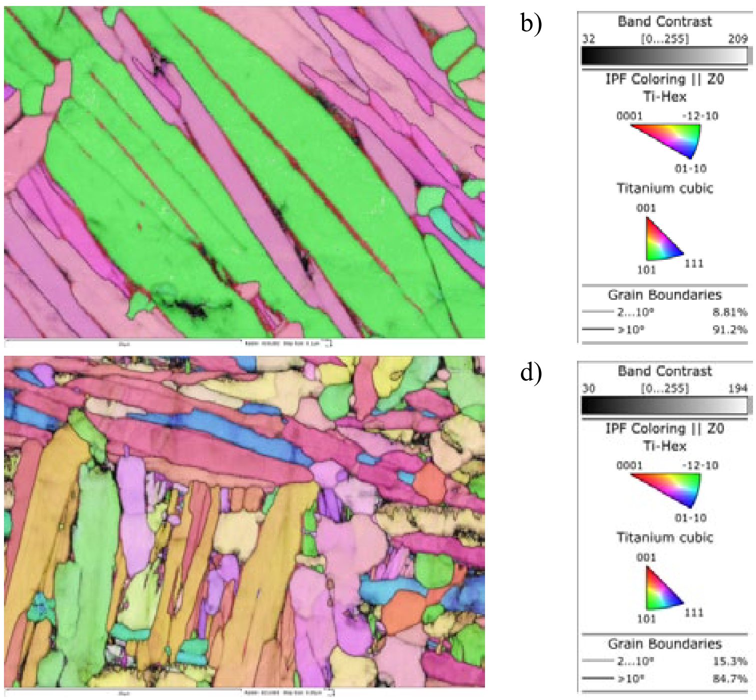

Fig. 15. EBSD/TKD-IPF orientation maps for α phase laths in Ti-6Al-4V alloy tempered at 900°C for 2 hours after WQ (a) and WQ + CC (c) – b,d) IPF color schemes for α and β phases

a)

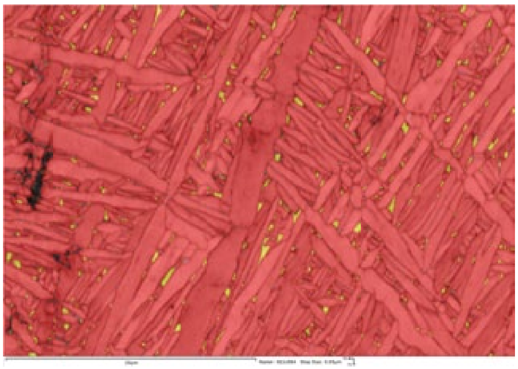

b)

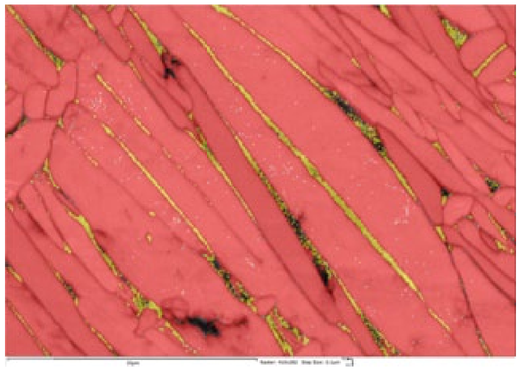

Fig. 16. EBSD/TKD phase composition maps of the WQ Ti-6Al-4V alloy after tempering at: a) 750°C, b) 900°C: red – α or α' phase, yellow – β phase

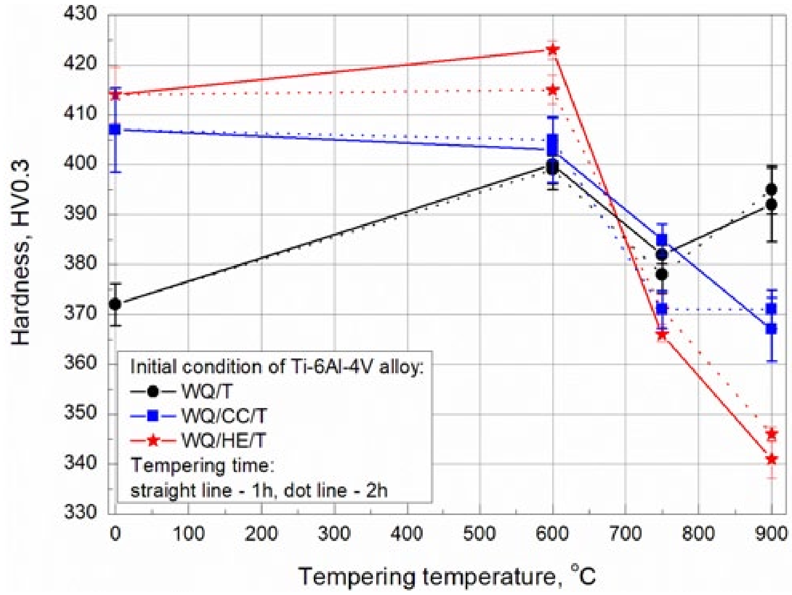

Fig. 17. The effect of tempering (T) on hardness of water quenched (WQ) and deformed (CC or HE) Ti-6Al-4V alloy

room temperature, this hardness increases to 407 HV (Fig. 17). A similar hardness – 414 HV – was obtained in water quenched and hydrostatically extruded alloy. Tempering at 600°C does not cause a significant change in the hardness of the quenched and plastically deformed alloys (WQ/CC and WQ/HE). In contrast, the hardness of the undeformed alloy increases – both after 1 and 2 hours of tempering. This is interesting because such tempering is not accompanied by a change in the morphology of the microstructural components (Fig. 13), and the expected effect is a reduction in the degree of supersaturation of the α-phase laths with alloying elements. Therefore, the possibility of Ti_3Al phase precipitation (Fig. 7b) [8,9,22-24] or the transformation of α" martensite into α' one [16] cannot be ruled out. The decrease in hardness of the alloy tempered at higher temperatures – 750 and 900°C – results from changes in the size and morphology of the α-phase laths and an increase in the relative volume of the β-phase (Fig. 16). The effect of plastic deformation of martensite on the hardness of the Ti-6Al-4V alloy after tempering at 900°C is difficult to assess due to the occurrence of the $\alpha + \beta \rightarrow \beta$ phase transformation. Differences in hardness result from the varying relative volume of the transformed β phase and the morphology of its components. After tempering at 900°C, the β phase content appears to be lowest in the undeformed alloy (Fig. 16b), hence its hardness (>390 HV) is higher than after quenching, and the highest compared to the WQ/CC (approx. 370 HV) and WQ/HE (<345 HV) conditions.

4. Conclusions

The formation and decomposition of martensite in two-phase titanium alloys is usually associated with conventional heat treatment – quenching and tempering. Previous studies have shown that the decomposition process proceeds differently under static and dynamic conditions – i.e. during plastic deformation. The aim of the present study was therefore to assess the influence of martensite deformation on the characteristics of its subsequent decomposition. Based on an analysis of the results obtained, the following conclusions can be formulated:

– martensite retains its lath-like morphology both after compression at room temperature and after hydrostatic extrusion at 600°C,

– dislocation substructures and twins were observed in martensite laths, regardless of the degree of their plastic deformation,
– martensite, both in the undeformed and deformed state, is chemically homogeneous,
– tempering at 600°C leads to the thickening of α-phase laths formed from both undeformed and deformed martensite,
– TEM analysis after tempering at 600°C of undeformed martensite revealed nanometer-size precipitates in α laths – it cannot be ruled out that these are Ti_3Al phase,
– dislocations appear to play an important role in shaping the microstructure at tempering temperature of 900°C, forming characteristic substructures – transforming into small-angle grain boundaries (SAGB's) in the laths formed as a result of the decomposition of deformed martensite,
– STEM/EDS analysis showed that the diffusion of alloying elements plays a significant role in the martensite decomposition in Ti-6Al-4V alloy. Tempering is associated with a reduction in the degree of martensite supersaturation, particularly with respect to the element stabilizing the β phase – i.e., V. Vanadium, diffusing outward from the α'(α") phase laths, contributes to the formation of the β phase between them,
– TKD analysis indicates a significant increase in the proportion of SAGB's (2-10°) – from 4.35% for the water quenched state to 31.7% after deformation,
– TKD phase composition maps confirmed that after tempering at 750 and 900°C, a β phase forms between the α phase crystallites,
– the presence of martensite in the microstructure of the alloy under study increases its hardness – from 342 to 373 HV,
– as a result of compression at room temperature and hydrostatic pressing at 600°C, martensite hardens to a value of 407 and 414 HV, respectively,
– tempering at 600°C of undeformed alloy leads to a significant increase in hardness, despite only a slight change in its microstructure – this may be due to the precipitation of the Ti_3Al phase or α" → α' transformation.

Acknowledgments

Thanks to Prof. Sergey Zherebtsov (Belgorod State University, Russia) for providing the water quenched and hydrostatically extruded material.

REFERENCES

[1] U. Zwicker, Titanium and Titanium Alloys. Springer-Verlag, Berlin (1974).
[2] G. Lutjering, J.C Williams, Titanium, Springer-Verlag, Berlin Heidelberg (2003).
[3] M. Motyka, K. Kubiak, J. Sieniawski, W. Ziaja, Phase transformation and characterization of α+β titanium alloys. In: S. Hashmi (Ed.), Comprehensive Materials Processing – Volume 2: Materials Modelling and Characterization, Elsevier (2014).
[4] M. Motyka, Thermomechanical Processing for Development of Phase Constituents Morphology and Plasticity of Two-Phase Titanium Alloys (in Polish). RUT Press, Rzeszow (2015).
[5] Y. Mantani, M. Tajima, Phase transformation of quenched α" martensite by aging in Ti-Nb alloys. Mater. Sci. Eng. A. **438-440**, 315-319 (2006).
DOI: https://doi.org/10.1016/j.msea.2006.02.180
[6] K. Sato, H. Matsumoto, K. Kodaira, T.J. Konno, A. Chiba, Phase transformation and age-hardening of hexagonal α' martensite in Ti-12 mass% V-2 mass% Al alloys studied by transmission electron microscopy, J. Alloy. Comp. **506**, 607-614 (2010).
DOI: https://doi.org/10.1016/j.jallcom.2010.07.127
[7] L. Zeng, T.R. Bieler, Effects of working, heat treatment, and aging on microstructural evolution and crystallographic texture of α, α',α" and α phases in Ti-6Al-4V wire. Mater. Sci. Eng. A. **392**, 403-414 (2005).
DOI: https://doi.org/10.1016/j.msea.2004.09.072
[8] F.X. Gil Mur, D. Rodríguez, J.A. Planell, Influence of tempering temperature and time on the α"-Ti-6Al-4V martensite. J. Alloys Compd. **234**, 287-289 (1996).
DOI: https://doi.org/10.1016/0925-8388(95)02057-8
[9] J.I. Qazi, O.N. Senkov, J. Rahim, F.H. Froes, Kinetics of martensite decomposition in Ti-6Al-4V-xH alloys. Mater. Sci. Eng. A. **359**, 137-149 (2003).
DOI: https://doi.org/10.1016/S0921-5093(03)00350-2
[10] S. Cao, R. Chu, X. Zhou, K. Yang, Q. Jia, C.V.S. Lim, A. Huang, X. Wu , Role of martensite decomposition in tensile properties of selective laser melted Ti-6Al-4V, J. Alloys Compd. **744**, 357-363 (2018). DOI: https://doi.org/10.1016/j.jallcom.2018.02.111
[11] C. de Formanoir, G. Martin, F. Prima, S.Y.P. Allain, T. Dessolier, F. Sun, , S. Vivès, B. Hary, Y. Bréchet, S. Godet, Micromechanical behavior and thermal stability of a dual-phase α+α' titanium alloy produced by additive manufacturing. Acta Mater. **162**, 149-162 (2019). DOI: https://doi.org/10.1016/j.actamat.2018.09.050
[12] A. Zafari, M.R. Barati, K. Xia, Controlling martensitic decomposition during selective laser melting to achieve best ductility in high strength Ti-6Al-4V. Mater. Sci. Eng. A. **744**, 445-455 (2019).
DOI: https://doi.org/10.1016/j.msea.2018.12.047
[13] H. Inagaki, Mechanism of enhanced superplasticity in thermomechanically processed Ti-6Al-4V. Z. Metallkd. **87**, 179-186 (1996).
[14] M. Motyka, J. Sieniawski, W. Ziaja, Microstructural aspects of superplasticity in Ti-6Al-4V alloy. Mater. Sci. Eng. A. **599**, 57-63 (2014). DOI: https://doi.org/10.1016/j.msea.2014.01.067
[15] X. Li, M. Sha, J. Chu, Compressive deformability of hardened titanium alloy VT16. Metal. Sci. Heat Treat. **51**, 594-598 (2009).
DOI: https://doi.org/10.1007/s11041-010-9217-6
[16] A.G. Illarionov, S.L. Demakov, S.I. Stepanov, S.M. Illarionova, Structural and phase transformations in a quenched two-phase titanium alloy upon cold deformation and subsequent annealing. Phys. Metals Metallogr. **116**, 267-273 (2015).
DOI: https://doi.org/10.1134/s0031918x15030060
[17] M. Motyka, A. Baran-Sadleja, J. Sieniawski, M. Wierzbińska, K. Gancarczyk, Decomposition of deformed α'(α") martensitic

phase in Ti-6Al-4V alloy. Mater. Sci. Tech. **35**, 260-272 (2019). DOI: https://doi.org/10.1080/02670836.2018.1466418

[18] P. Barriobero-Vila, V.B. Oliveira, S. Schwarz, T. Buslaps, G. Requena, Tracking the α" martensite decomposition during continuous heating of a Ti-6Al-6V-2Sn alloy. Acta Mater. **135**, 32-143 (2018). DOI: https://doi.org/10.1016/j.actamat.2017.06.018

[19] X. Tan, Y. Kok, W.Q. Toh, Y.J. Tan, M. Descoins, D. Mangelinck, S.B. Tor, K.F. Leong, C.K. Chua, Revealing martensitic transformation and α/β interface evolution in electron beam melting three-dimensional-printed Ti-6Al-4V. Sci. Rep. **6**, 26039 (2016). DOI: https://doi.org/10.1038/srep26039

[20] S. Zherebsov, A. Mazur, G. Salishchev, W. Łojkowski: Effect of hydrostatic extrusion at 600–700°C on the structure and properties of Ti–6Al–4V alloy. Mater. Sci. Eng. A. **485**, 39-45 (2008). DOI: https://doi.org/10.1016/j.msea.2007.08.081

[21] E. Farabi, V. Tari, P.D. Hodgson, G.S. Rohrer, H. Beladi: On the grain boundary network characteristics in a martensitic Ti–6Al–4V alloy. J. Mater. Sci. **55**, 15299-15321 (2020). DOI: https://doi.org/10.1007/s10853-020-05075-7

[22] Y. Vahidshad, A.H. Khodabakhshi: Effect of solution treatment and aging temperature on α′ and $Ti_3Al(\alpha_2)$ phase formation and mechanical properties of water-quenched Ti-6Al-4V. Metallogr. Microstruct. Anal. **11**, 59-71 (2022). DOI: https://doi.org/10.1007/s13632-021-00818-7

[23] B. Callegari, J.V. Marçola, K. Aristizabal, F.A. Soldera, F. Mücklich, H.C. Pinto: Effect of microstructure on Ti_3Al precipitation during ageing of Ti-6Al-4V alloy. MATEC Web Conf. **321**, 12014 (2020). DOI: https://doi.org/10.1051/matecconf/202032112014

[24] D. Lee, S. Lee, Effects of nano-sized α_2 (Ti_3Al) particles on quasi-static and dynamic deformation behavior of Ti-6Al-4V alloy with bimodal microstructure. J. Mater. Sci. **40**, 4077-4084 (2005). DOI: https://doi.org/10.1007/s10853-005-1914-y

[25] A. Janda, S. Ebenbauer, A. Prestl, I. Siller, H. Clemens, P. Spoerk-Erdely, In-situ hightemperature EBSD characterization during a solution heat treatment of hot-rolled Ti-6Al-4V. Mater. Charact. **192**, 112207 (2022). DOI: https://doi.org/10.1016/j.matchar.2022.112207

[26] M. Sozańska, B. Chmiela, Ocena możliwości stosowania metody EBSD w badaniach mikrostruktury stopów tytanu. Inżynieria Materiałowa **33**, 311-314 (2021).

[27] G.S. Dyakonov, E. Zemtsova, S. Mironov, I.P. Semenova, R.Z. Valiev, S.L. Semiatin, An EBSD investigation of ultrafine-grain titanium for biomedical applications. Mater. Sci. Eng., A. **648**, 305-310 (2015). DOI: https://doi.org/10.1016/j.msea.2015.09.080

[28] H. Beladi, Q. Chao, G.S. Rohrer, Variant selection and intervariant crystallographic planes distribution in martensite in a Ti–6Al–4V alloy. Acta Mater. **80**, 478-489 (2014). DOI: https://doi.org/10.1016/j.actamat.2014.06.064